C. R. Mecanique 347 (2019) 663–675

Contents lists available at ScienceDirect

Comptes Rendus Mecanique

www.sciencedirect.com

Gear fault diagnosis under non-stationary operating mode based on EMD, TKEO, and Shock Detector

Ridha Ziani [a,*], Ahmed Hammami [b], Fakher Chaari [b], Ahmed Felkaoui [a], Mohamed Haddar [b]

[a] Laboratory of Applied Precision Mechanics, Institute of Optics and Precision Mechanics, Ferhat Abbes University Sétif 1, Sétif 19000, Algeria
[b] Laboratory of Mechanics, Modeling and Production, National School of Engineers of Sfax, BP 1173, 3038 Sfax, Tunisia

ARTICLE INFO

Article history:
Received 16 May 2019
Accepted 8 August 2019
Available online 9 September 2019

Keywords:
Fault diagnosis
Signal processing
Vibration
EMD
TKEO
Shock Detector

ABSTRACT

Condition monitoring of gearboxes running under non-stationary operating conditions is a very difficult task. In this study, a signal processing technique is developed for damage detection of a bevel gearbox running under variable load and speed conditions. The proposed technique is applied on simulated vibration data computed through a dynamic model of bevel gearbox. The procedure used in this technique is based on the extraction of the shock related to the defect using the Shock Detector (SD) method. Firstly, vibration signals are decomposed into IMFs using Empirical Mode Decomposition (EMD). Then, the Teager–Kaiser Energy Operator (TKEO) is used to assess the instantaneous energy of the signal. Afterwards, SD is applied to examine and quantify the shock contents of the TKEO signal, which reflect the effect of the defect.

1. Introduction

The non-stationary regimes correspond to the operating states of a rotating machine with variations of its rotating speed, mainly generated by start-up procedures, load change conditions, and operating disturbances. Fault diagnosis of gearboxes operating under non-stationary modes is a particular challenge that has attracted considerable attention of researchers in recent years.

Vicuña and Chaari [1] stated that in non-stationary conditions, caused generally by load and speed fluctuations, the classical signal processing techniques such as pure spectral analysis are inefficient to diagnose the machine defects. To overcome this problem, time-frequency analysis offers the possibility of representing in these two spaces the non-stationary signals. In this category, Short Time Fourier Transform (STFT), operation from which is determined the spectrogram, was widely applied for fault diagnosis running in stationary and non-stationary modes [2–5]. Worden et al. [6] indicate that the major limitation of STFT analysis lies in the trade-off considered between the two dimensions in terms of resolution. A good localization in time involves the use of a small window, which leads consequently to a poor frequency resolution and vice versa.

* Corresponding author.
E-mail address: ridha.ziani@univ-setif.dz (R. Ziani).

https://doi.org/10.1016/j.crme.2019.08.003
1631-0721/

Table 1
Model characteristics of the bevel transmission [20].

	Pinion	Wheel
Teeth numbers	14	45
Module (mm)	9	
Spiral angle (rad)	0.480	
Pitch angle (rad)	0.302	1.269
Pitch radius (m)	0.067	0.215
Face width (m)	0.064	
Mass (kg)	24.71	122.67
Torsional moment of inertia (kg·m^2)	0.0585	1.91
Bending moment of inertia (kg·m^2)	0.501	2.07
Rotation speed (rpm)	1320	410
Axial support stiffness (N/m)	1.0E9	2.3E9
Lateral support stiffness (N/m)	8.8E9	1.3E10
Torsional stiffness of shaft (Nm/rad)	1.2E4	7.4E4
Bending shaft-bearing stiffness (Nm/rad)	3.1E7	9.8E7
Mesh damping ratio	0.06	
Support component damping ratio	0.02	
Gear backlash (mm)	0.1	
Pressure angle	$\alpha = 20°$	

The Wigner–Ville distribution constitutes another signal processing technique used in time frequency analysis [7] and can evaluate how the frequency components of signals evolve over time, but the main disadvantage associated with this distribution is its lack of readability caused by the presence of interference terms that have no physical reality and can hide the physically significant components.

Wavelet decomposition or time-scale analysis represent another category of signal processing techniques used for non-stationary signals analysis [8–10]. Other advanced approaches were recently developed such as cyclostationary analysis [2], and Empirical Mode Decomposition (EMD) [11–14].

In addition, the Hilbert–Huang transform (HHT) is a condition monitoring method based on the combination of the empirical mode decomposition (EMD) and the Hilbert spectral analysis (HSA) [15]. This method can be adopted to detect the presence of defects without identification of fault pattern [16].

For a gear transmission, a local defect leads to a diminution in the stiffness of the faulty tooth [17] which generates periodic impulses components in the vibration signal. We propose in this paper to diagnose such defect and track impulses for a gearbox running under variable load and speed conditions. Simulated signals generated from a dynamic model of a bevel gearbox are decomposed using EMD, which allows getting a number of Intrinsic Modes Functions (IMFs). Since the first IMFs are known for the wealth of information they convey [18], the procedure that follows will be applied only to the first four IMFs.

In order to detect shocks in the IMF signals, which are generally considered as reflecting the presence of defects, we use a technique called Shock Detector (SD). This technique, based on the assessment of the energy level of windows shock filters, was successfully applied by Badri et al. [19] to detect bearing slipping and was also used for multiple damage diagnosis. The main advantage of SD technique is that it has no analytical formulation and can isolate shocks and quantify their energy contents in the signal. This technique was never implemented for monitoring and diagnosing gearbox operating in non-stationary mode.

In this paper, we proposed to use the Shock Detector technique in order to detect tooth defect in a bevel gearbox. The tool used for evaluating the energy level of shocks will be in the case studied here the Teager–Kaiser Energy Operator (TKEO). This paper is organized in the following order: in the second section, a dynamic model of the gearbox is presented. The third section describes the proposed fault diagnosis procedure. The fourth section presents the obtained results. Finally, a conclusion is given in the fifth section.

2. Dynamic model of a spiral bevel gearbox

The proposed fault diagnosis method is evaluated using simulated vibration data generated from a dynamic model of bevel gearbox as illustrated in Fig. 1. This transmission is operating under simultaneous speed and load variation and composed mainly of a motor coupled with the gearbox [18,20].

The characteristics of this model are given in Table 1.

The equation of motion of this model is established by using Lagrange formalism [21]:

$$M\ddot{q} + C\dot{q} + K(t)q = F \tag{1}$$

The degree of freedom vector is defined as:

$$q = \{x_1, y_1, z_1, \theta_m, \theta_1, x_2, y_2, z_2, \theta_2, \theta_r\}^{\mathsf{T}} \tag{2}$$

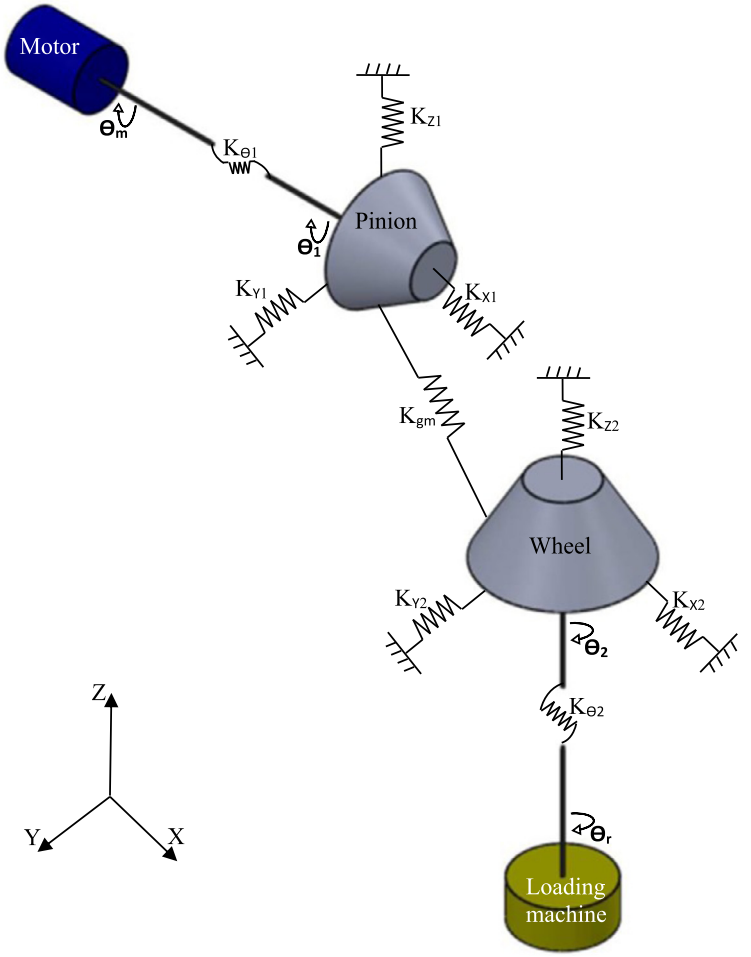

Fig. 1. Dynamic model of bevel gear transmission.

The mass matrix **M** is defined as:

$$M = \mathrm{diag}\,(m_1, m_1, m_1, I_m, I_1, m_2, m_2, m_2, I_2, I_r) \tag{3}$$

m_1 and m_2 are respectively the mass of the first and of the second block. I_{m}, I_{r}, I_1, I_2 are respectively the inertia moment of the motor, the receiver, the pinion, and the wheel gear.

The stiffness matrix $K(t)$ is defined as:

$$K(t) = \begin{bmatrix}
s_2k_{\mathrm{e}} + k_{x_1} & -s_6k_{\mathrm{e}} & -s_4k_{\mathrm{e}} & 0 & -s_9k_{\mathrm{e}} & -s_2k_{\mathrm{e}} & s_6k_{\mathrm{e}} & s_4k_{\mathrm{e}} & s_{10}k_{\mathrm{e}} & 0 \\
-s_6k_{\mathrm{e}} & s_3k_{\mathrm{e}} + k_{y_1} & s_5k_{\mathrm{e}} & 0 & s_{11}k_{\mathrm{e}} & s_6k_{\mathrm{e}} & -s_3k_{\mathrm{e}} & -s_5k_{\mathrm{e}} & -s_{12}k_{\mathrm{e}} & 0 \\
-s_4k_{\mathrm{e}} & s_5k_{\mathrm{e}} & s_1k_{\mathrm{e}} + k_{z_1} & 0 & s_7k_{\mathrm{e}} & s_4k_{\mathrm{e}} & -s_5k_{\mathrm{e}} & -s_1k_{\mathrm{e}} & -s_8k_{\mathrm{e}} & 0 \\
0 & 0 & 0 & k_{\theta_1} & -k_{\theta_1} & 0 & 0 & 0 & 0 & 0 \\
-s_9k_{\mathrm{e}} & s_{11}k_{\mathrm{e}} & s_7k_{\mathrm{e}} & -k_{\theta_1} & k_{\theta_1} + s_{13}k_{\mathrm{e}} & s_9k_{\mathrm{e}} & -s_{11}k_{\mathrm{e}} & -s_7k_{\mathrm{e}} & -s_{15}k_{\mathrm{e}} & 0 \\
-s_2k_{\mathrm{e}} & s_6k_{\mathrm{e}} & s_4k_{\mathrm{e}} & 0 & s_9k_{\mathrm{e}} & s_2k_{\mathrm{e}} + k_{x_2} & -s_6k_{\mathrm{e}} & -s_4k_{\mathrm{e}} & -s_{10}k_{\mathrm{e}} & 0 \\
s_6k_{\mathrm{e}} & -s_3k_{\mathrm{e}} & -s_5k_{\mathrm{e}} & 0 & -s_{11}k_{\mathrm{e}} & -s_6k_{\mathrm{e}} & s_3k_{\mathrm{e}} + k_{y_2} & -s_5k_{\mathrm{e}} & -s_{12}k_{\mathrm{e}} & 0 \\
s_4k_{\mathrm{e}} & -s_5k_{\mathrm{e}} & -s_1k_{\mathrm{e}} & 0 & -s_7k_{\mathrm{e}} & -s_4k_{\mathrm{e}} & -s_5k_{\mathrm{e}} & s_1k_{\mathrm{e}} + k_{z_2} & s_8k_{\mathrm{e}} & 0 \\
s_{10}k_{\mathrm{e}} & -s_{12}k_{\mathrm{e}} & -s_8k_{\mathrm{e}} & 0 & -s_{15}k_{\mathrm{e}} & -s_{10}k_{\mathrm{e}} & s_{12}k_{\mathrm{e}} & s_8k_{\mathrm{e}} & k_{\theta_2} + s_{14}k_{\mathrm{e}} & -k_{\theta_2} \\
0 & 0 & 0 & 0 & 0 & 0 & 0 & 0 & -k_{\theta_2} & k_{\theta_2}
\end{bmatrix} \tag{4}$$

K_{x_i}, K_{y_i}, and K_{z_i} $(i = 1, 2)$ are the bearing stiffness of each block. K_{θ_i} $(i = 1, 2)$ are the torsional stiffnesses of the shafts. The terms s_j $(j = 1..12)$ are defined in Table 2, where $a_1 = \sin\alpha \sin\delta_1 + \cos\alpha \sin\beta \cos\delta_1$, $a_2 = \sin\alpha \cos\delta_1 - \cos\alpha \sin\beta \sin\delta_1$, $a_3 = \cos\alpha \cos\beta$. β is the spiral angle, δ_1 is the gear pitch angle and α is the pressure angle. r_{m_1} and r_{m_2} are respectively the mean radius of the pinion and the wheel gear.

Table 2
s_j terms.

$s_1 = (a_3)^2$	$s_6 = a_1 \cdot a_2$	$s_{11} = r_{m_1} \cdot a_2 \cdot a_3$
$s_2 = (a_1)^2$	$s_7 = r_{m_1}(a_3)^2$	$s_{12} = r_{m_2} \cdot a_2 \cdot a_3$
$s_3 = (a_1)^2$	$s_8 = r_{m_2}(a_3)^2$	$s_{13} = (r_{m_1})^2(a_3)^2$
$s_4 = a_1 \cdot a_3$	$s_9 = r_{m_1} \cdot a_1 \cdot a_3$	$s_{14} = (r_{m_2})^2(a_3)^2$
$s_5 = a_2 \cdot a_3$	$s_{10} = r_{m_2} \cdot a_1 \cdot a_3$	$s_{15} = r_{m_1} \cdot r_{m_2} \cdot (a_3)^2$

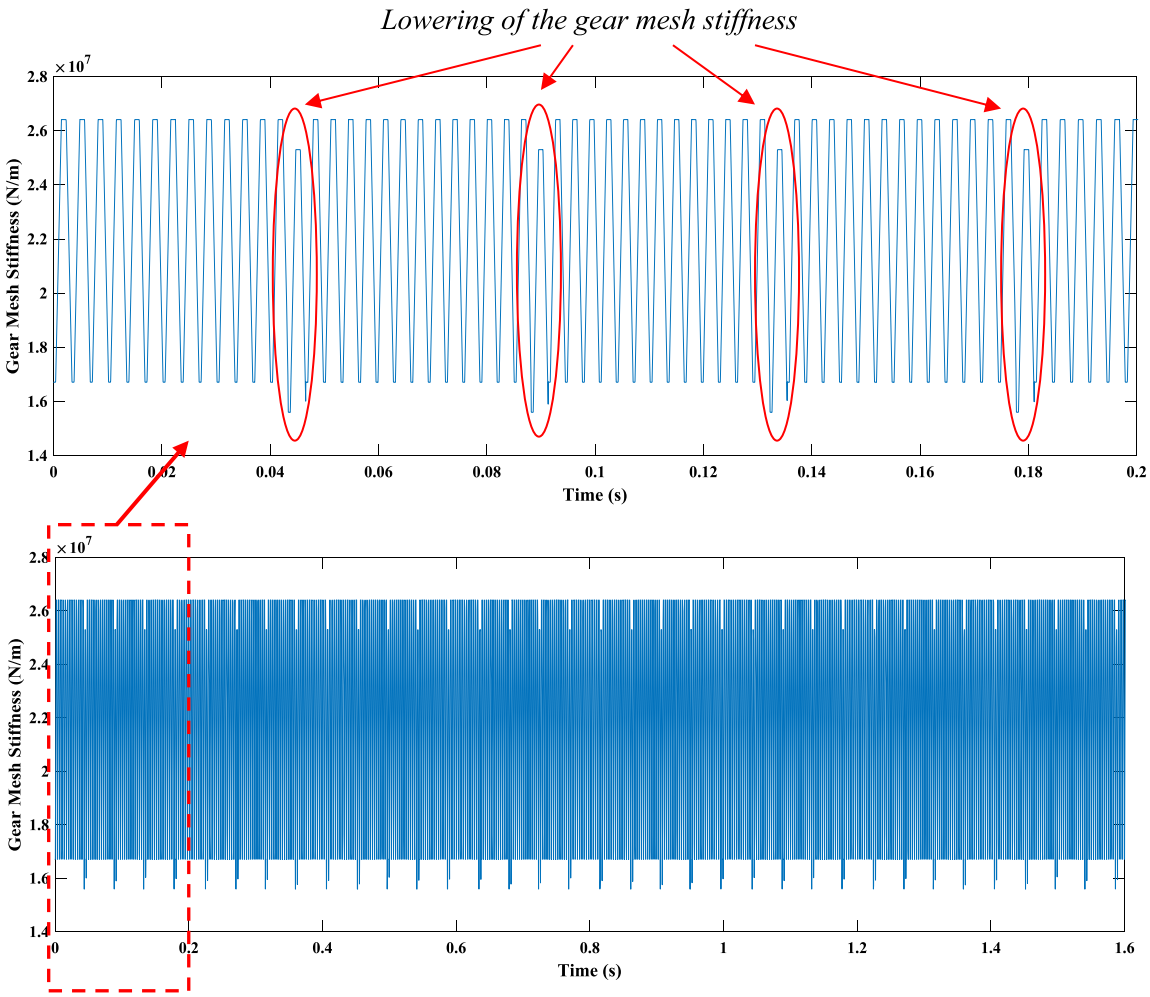

Fig. 2. Time evolution of the gear mesh stiffness.

K_e is the gear mesh stiffness that is presented in Fig. 2. This stiffness is modeled as a trapezoidal function taking into account the rotational speed variation and the cracked defect, which is modeled by the lowering of the gear mesh stiffness when the defected tooth is in contact.

The proportional damping matrix is:

$$C = 0.05M + 10^{-4}\overline{K} \tag{5}$$

$\overline{K}$ is the mean stiffness matrix of $K(t)$. The external force vector is defined as:

$$F = \{0, 0, 0, C_m, 0, 0, 0, 0, 0, C_r\}^{\intercal} \tag{6}$$

C_m and C_r are respectively the driving and the loading torque.

The equation of motion is computed through Newmark's algorithm [21].

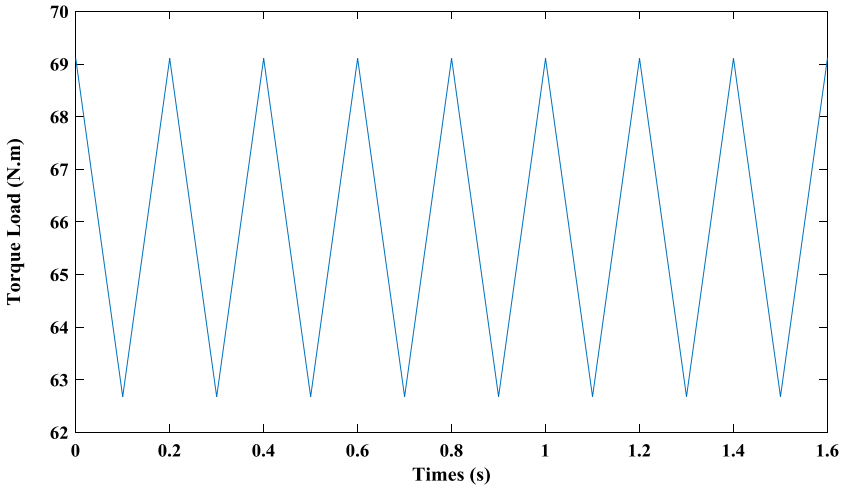

Fig. 3. Torque load variation shape.

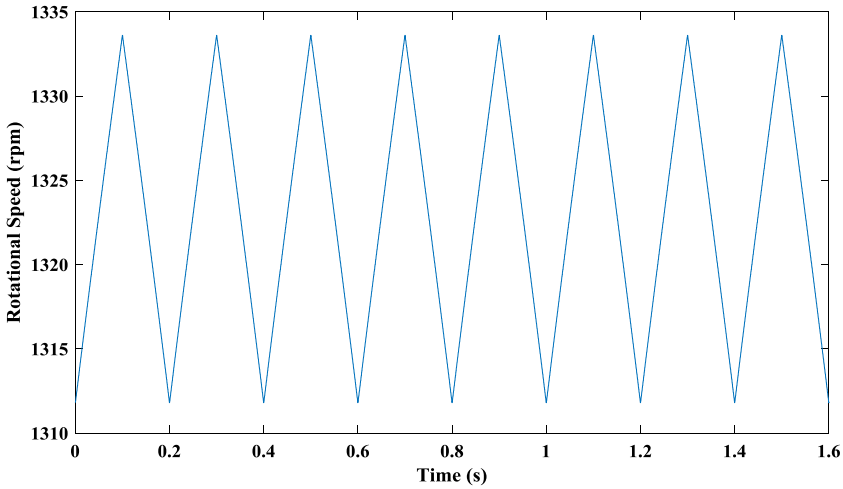

Fig. 4. Shape of the rotational speed variation.

As illustrated in Fig. 3, a torque of sawtooth profile with a periodic fluctuation of 0.2 s is used to load the gear transmission. This fluctuation of the load leads consequently to a fluctuation of the rotational speed shape as presented in Fig. 4.

The mean value of the rotational speed of the motor is $N = 1320$ rpm, which corresponds to a meshing frequency $f_m = 308$ Hz. In this model, a local defect (a crack) is considered on one tooth of the pinion. The defect period is $T_d = 0.045$ s, which corresponds to a defect frequency $f_d = 22$ Hz.

3. Procedure for gear fault detection

The proposed gear fault diagnosis procedure consists in decomposing the vibration signal into IMFs. The IMF having the highest kurtosis value is chosen for further processing. Afterwards, SD is used to follow shocks components in the selected IMF and to separate them from any other periodic component. SD uses three adjacent sliding windows on the time signal of the IMF. Then the following decision rule is adopted [19]:

- ➢ if the window centered on the sample i of the IMF has a kurtosis value that is greater than the one of its two left and right adjacent windows, the presence of a shock is declared. In this case, the shock filter takes the value of the central window's peak amplitude;
- ➢ otherwise, a null value is assigned to the shock filter.

In [19], authors used kurtosis to provide a measure of the energy inside each window, and then compare it to the ones of the adjacent windows. However, this descriptor is generally used to quantify the peakedness of a given signal [22]

and cannot provide precise information about the signal energy. Thus, we propose, in this paper, to keep the same rule of decision about the presence of the shock but to use the sum of the instantaneous energy instead of the kurtosis to quantify the energy inside each window.

The bevel gear transmission model presented in section 2 is subjected to simultaneous fluctuations of load and speed. These fluctuations lead consequently to both Amplitude and Frequency Modulation (AM-FM) of the vibration signal so that EMD is no longer efficient and needs further processing. In order to overcome this problem of modulation, we use the Teager–Kaiser Energy Operator (TKEO). On the one hand, TKEO is a suitable tool for demodulation purpose [21]; on the other hand, this operator computes the instantaneous energy of the signal, which facilitates shock detection by comparing directly the instantaneous energy inside the three windows of SD. In what follows, we will provide a brief overview of the three implemented techniques, i.e. EMD, SD, and TKEO.

3.1. Empirical Mode Decomposition (EMD)

EMD, developed originally by Huang et al. [23], is designed to work well for non-stationary signals. This technique was commonly practically used for the diagnostic of rotating machines in non-stationary operating mode. The EMD technique consists in decomposing any signal $x(t)$ into a reduced number of IMFs as follows:

$$x(t) = \sum_{i=1}^{n} IMF_i(t) + r(t) \tag{7}$$

where $r(t)$ is the obtained residue and n is the number of IMFs.

EMD is based on the following process; firstly, local maxima and minima are identified in the signal. Then all local maxima are connected by interpolation (cubic splines) to produce an upper envelope and all the minima are connected as a lower envelope. Afterwards, the mean of both envelopes is estimated and subtracted from the signal [24]. The result is declared as an IMF if certain criteria are satisfied. More details about EMD algorithm can be found in [23,24].

The IMF of a signal is always a mono-component AM–FM signal and thus we proposed, in this paper, to use TKEO for the demodulation task.

3.2. Teager Kaiser Energy Operator (TKEO)

TKEO was originally developed by Kaiser [25] for tracking the "energy" in speech signals, and has been extended to the entire class of signals. One of the well-known applications of TKEO is the analysis of speech signals, which are oscillatory signals with variable amplitude and frequency as functions of time [26]. The discrete TKEO consists in calculating instantaneous energy $xx(i)$ of the sampled signal $x(i)$ using the following formula:

$$xx(i) = x(i)^2 - x(i+1) \times x(i-1) \tag{8}$$

where i is the number of samples.

3.3. Shock Detector (SD)

As presented in [19], SD consists in scanning the sampled time signal using three adjacent windows of $2n+1$ samples (Fig. 5). At each position (i), SD computes the kurtosis value (replaced in this paper by the instantaneous energy of TKEO) of the central window C centered on i and then compare it to the ones of the adjacent left and right windows.

In this paper, SD is used to examine and quantify the shock contents of the TKEO signal of the most impulsive IMF. The size of the three windows is defined by considering the impact of the defect and the acquisition parameters, mainly the sampling frequency. Generally, when a defect occurs on one tooth of the gear, impulse components corresponding to the fault appear in the time signal, with a period corresponding to the rotation period. Hence the size of each window is chosen to be 1/3 of the rotation period:

$$W_{\text{length}} = \frac{1}{3 \times f_r} = (2n+1) \times \frac{1}{f_s} \tag{9}$$

where f_r and f_s are the rotation frequency and the sampling frequency respectively. n is the number of samples. Consequently, the number of samples in each window is given by:

$$N = 2n+1 = \frac{f_s}{3 \times f_r} \tag{10}$$

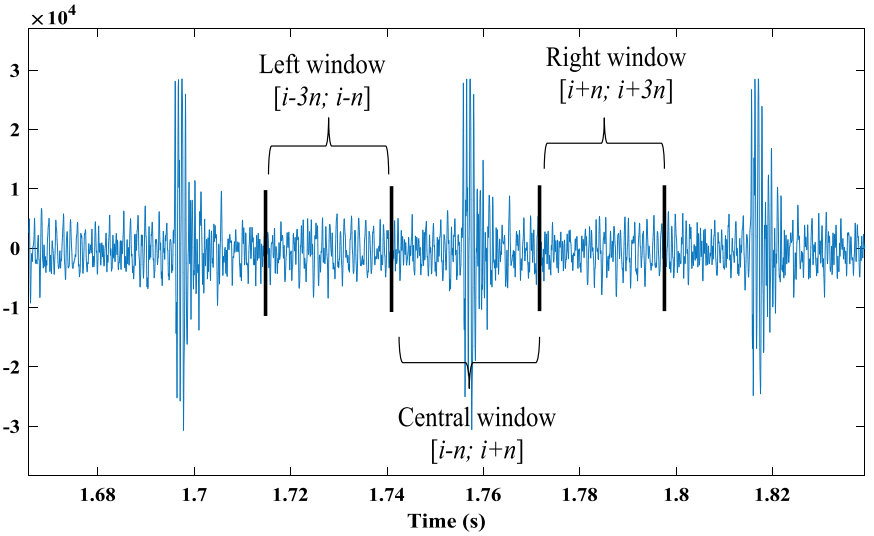

Fig. 5. Identification of shock windows.

4. Results and discussion

The aptitude of the proposed procedure to detect gear defect is evaluated using vibration signals simulated using the dynamic model of gear transmission presented in section 2.

Vibration signals are simulated from the above model in healthy and faulty conditions. A crack on one pinion of 14 teeth is introduced in the model as a repeated diminution in the profile of mesh stiffness when the defective tooth is in contact during the meshing process. A good impulse component extraction method should be generally robust to rotational speed fluctuation and defect severity. Therefore, the effectiveness of the proposed method is examined under rotational speed variation caused by load change and for different tooth severity levels: healthy gear, defect of level 1 (1% loss in mesh stiffness), and defect of level 2 (5% loss in mesh stiffness). The defect has a period of 0.045 s, corresponding to a frequency of 22 Hz.

By considering a sampling frequency of 30800 Hz and a rotation frequency of 22 Hz, we obtain $N = 467$ samples in each window of the Shock detector.

Fig. 6 shows times acceleration signals on pinion bearing for respectively healthy gear, defect of level 1, and defect of level 2. All signals are acquired under rotational speed fluctuation of 5%. The length of each signal is 1.626 s, with a transient phase of about 0.6 s.

Figs. 7, 8, and 9 show the EM decomposition of previous time series. For the three cases, it was observed that the second IMF has the highest kurtosis value. Thus it is chosen to be processed using TKEO.

Figs. 10, 11, and 12 show the TKEO signals applied to the second IMF obtained by EMD for the healthy gear, the first level of defect, and the second level of defect, respectively. In each figure, the shock detector filter is represented in red color. When a shock is present, the shock filter takes the value of the peak amplitude of the TKEO signal; otherwise, the shock filter takes a null value.

Finally, Figs. 13, 14, and 15 show the shock signals energy evolution for three cases of the study. For the healthy case (Fig. 13), and considering only the steady-state regime ($t > 0.6$ s), which in non-stationary, no shock components are detected, excepted for some impulsions that have no signification and can be related to noise. In Fig. 14, even though the defect level is relatively small (1%), the proposed method has successively tracked shocks components and isolated them. In this figure, periodic shock impulses due to the fault are clearly observed and have the corresponding fault period $\underline{T}_d = 0.45$ s. These periodic shocks are clearer in the shock signal for defect level 2 presented in Fig. 15.

In order to examine the robustness of this diagnosis procedure, three levels of defect (1%, 5%, and 10%) were considered, with an important rotational speed fluctuation of 50%. Fig. 16 show results of the proposed method with defect level 1 and 50% of rotational speed fluctuation.

In this figure, shocks corresponding to the fault are not very clear due to the important fluctuation of speed fluctuation, which masks the shock content corresponding to this lower level of defect. However, impulsions due the rotational speed fluctuation of period 0.2 s can be observed. In Figs. 17 and 18, with 50% of rotational speed fluctuation, shock impulsions due to the defect are correctly detected and isolated by the proposed method for both levels of defect (5% and 10%).

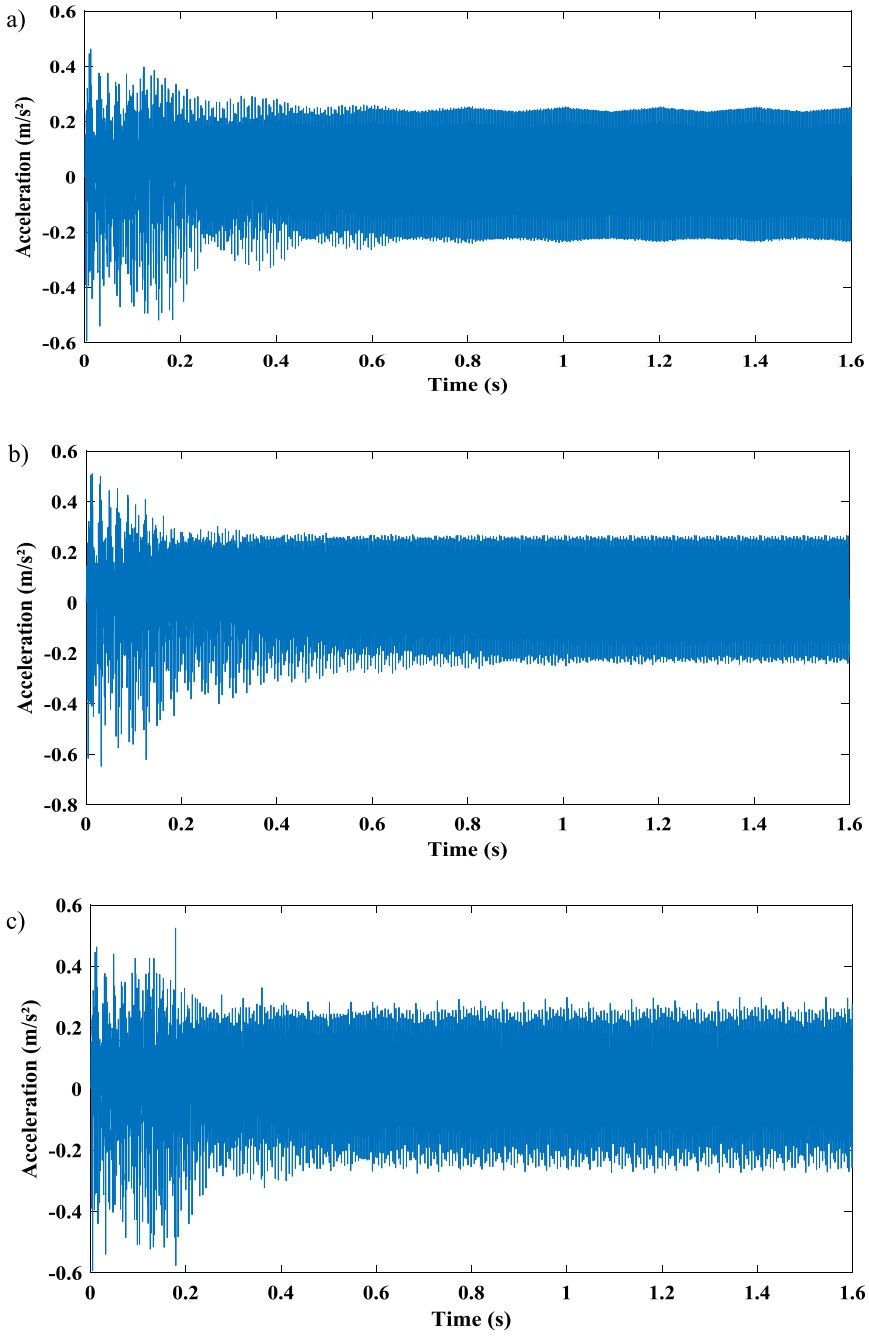

Fig. 6. Acceleration signals under 5% of rotational speed fluctuation: a) healthy conditions, b) defect level 1, c) defect level 2.

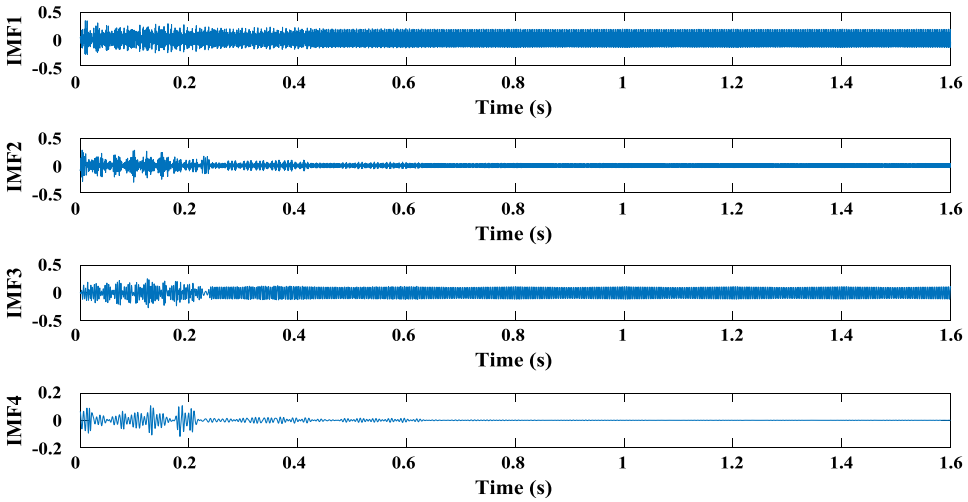

Fig. 7. EMD of the acceleration signal for a healthy gear.

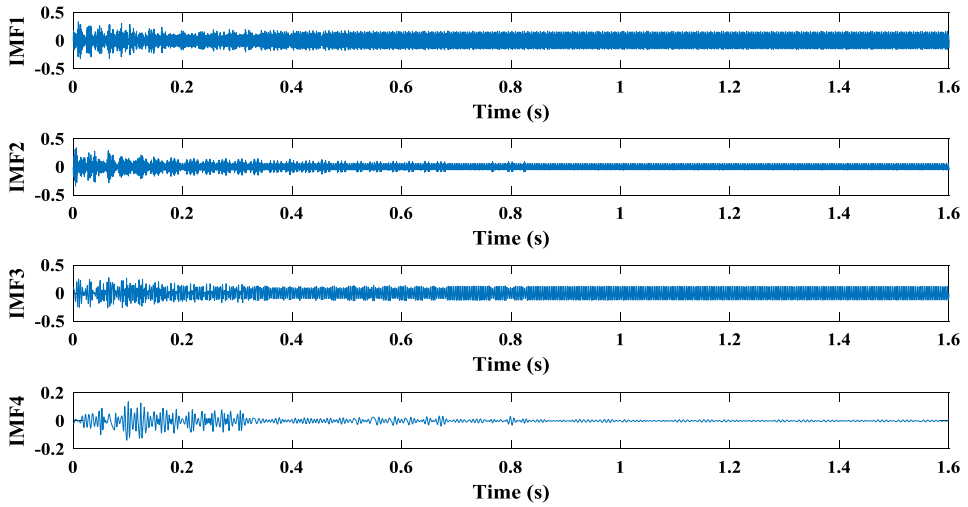

Fig. 8. EMD of the acceleration signal for defect level 1.

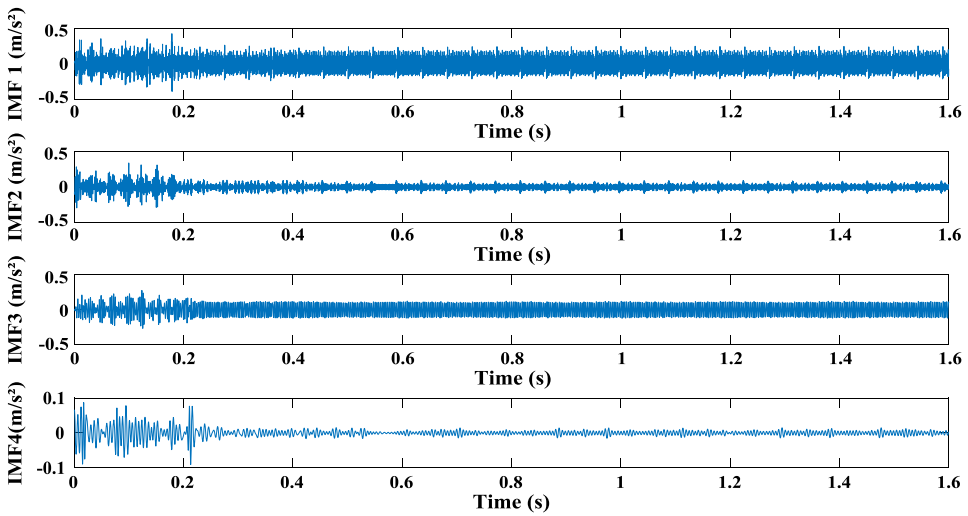

Fig. 9. EMD of the acceleration signal for defect level 2.

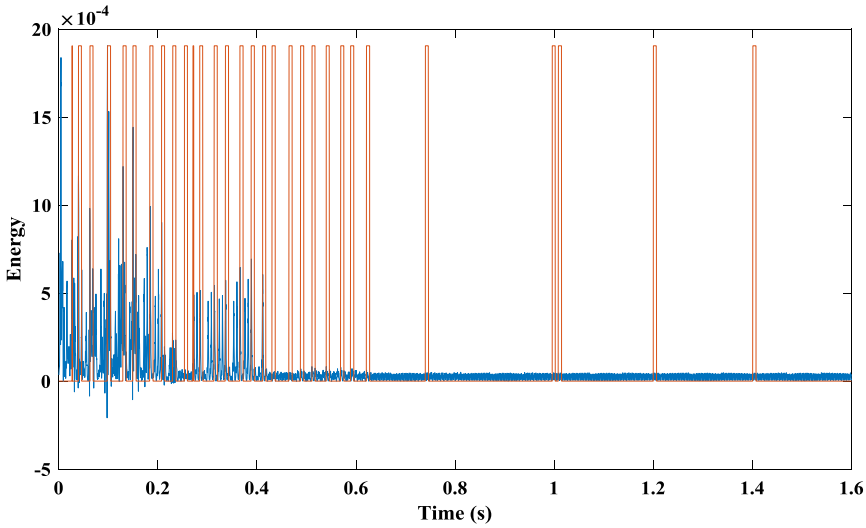

Fig. 10. TKEO of the 2nd IMF for a healthy gear and SD filter calculation.

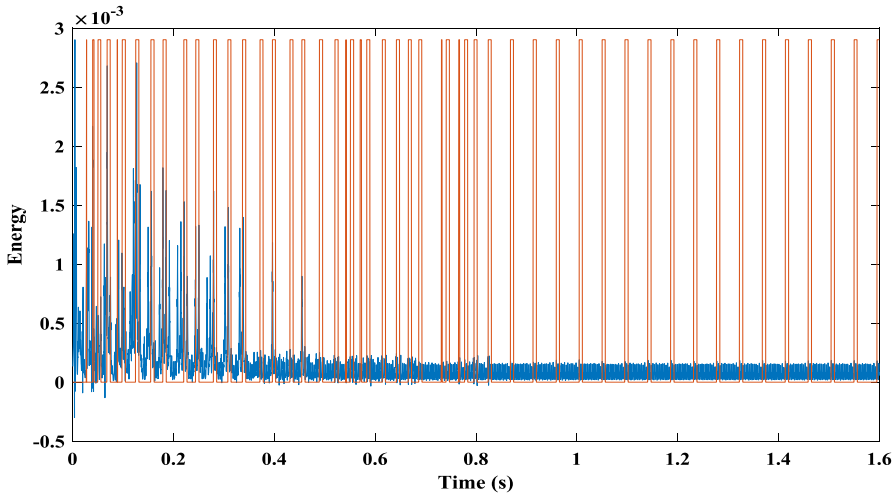

Fig. 11. TKEO of the 2nd IMF for defect level 1 and SD filter calculation.

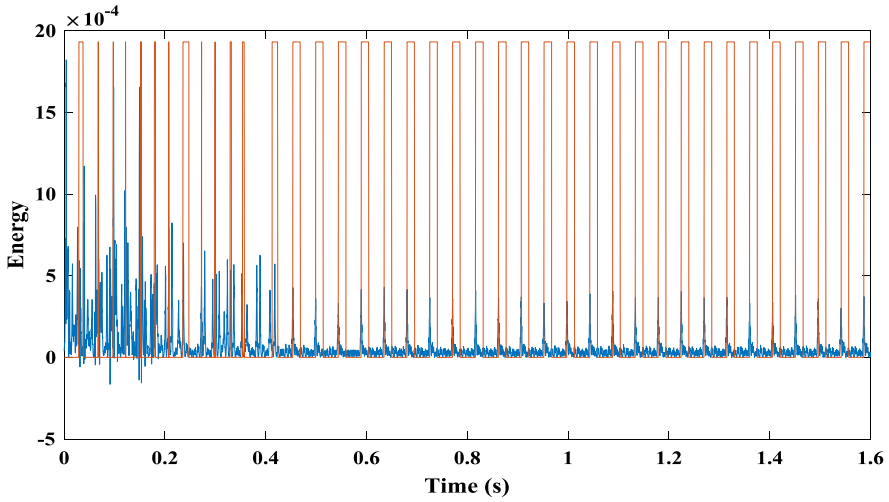

Fig. 12. TKEO of the 2nd IMF for defect level 2 and SD filter calculation.

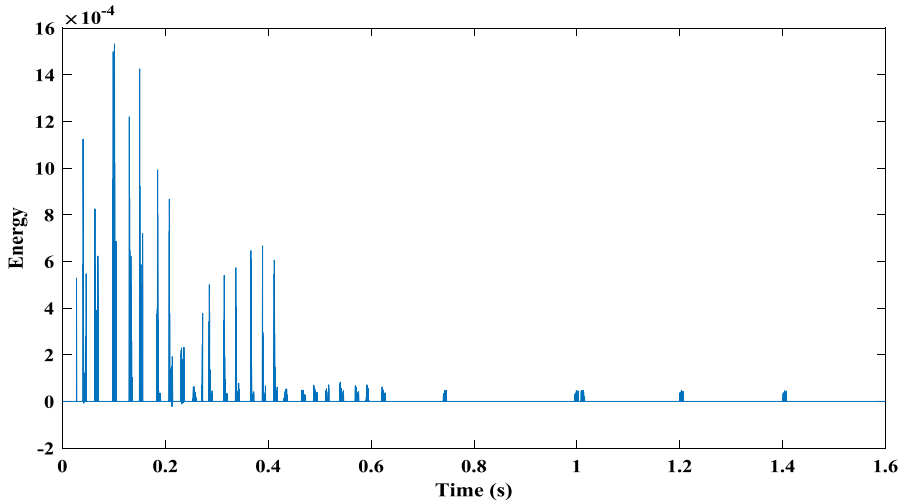

Fig. 13. Shock signal for a healthy gear.

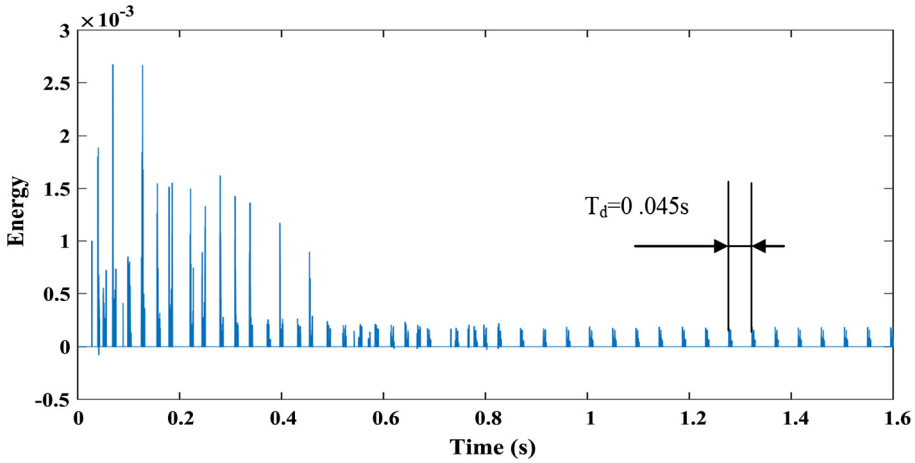

Fig. 14. Shock signal for defect level 1.

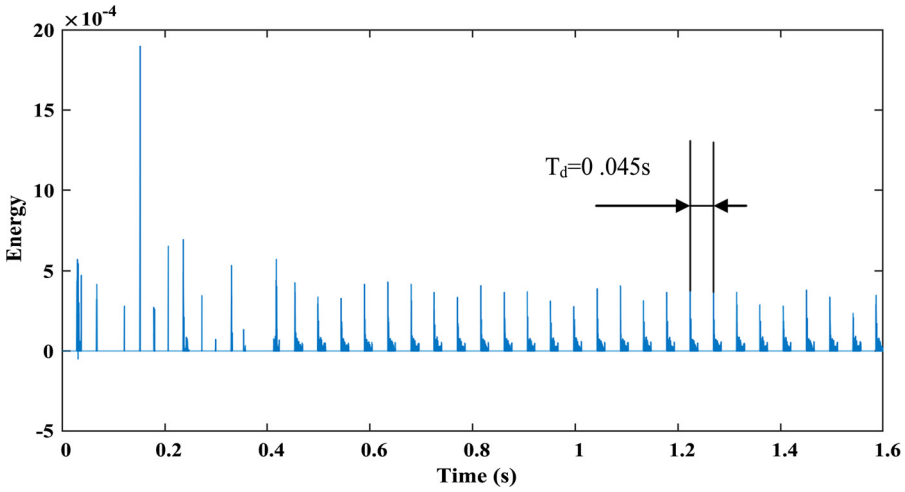

Fig. 15. Shock signal for defect level 2.

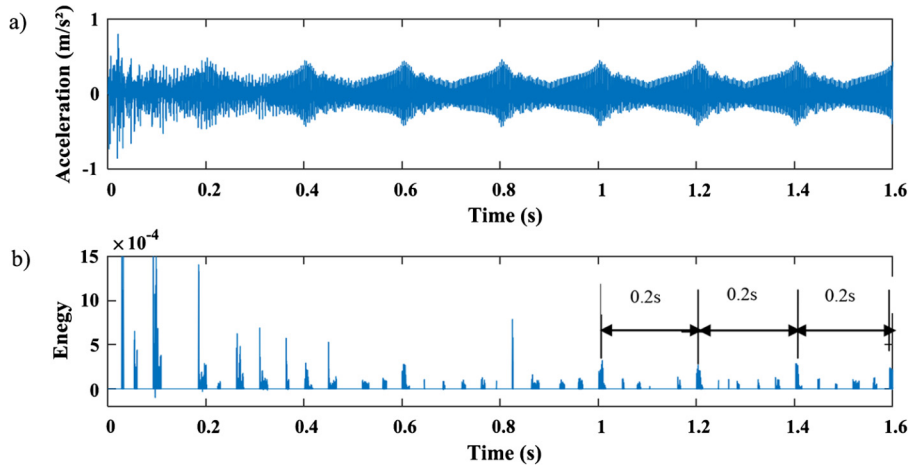

Fig. 16. Vibration signals of defect level 1 (1%) with 50% of rotational speed fluctuation: a) original signal; b) shock signal.

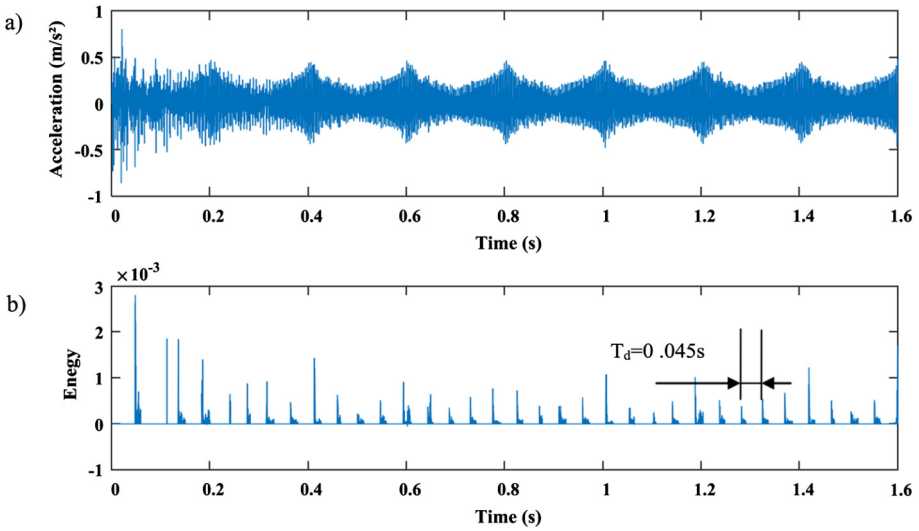

Fig. 17. Vibration signals of defect level 2 (5%) with 50% of rotational speed fluctuation: a) original signal; b) shock signal.

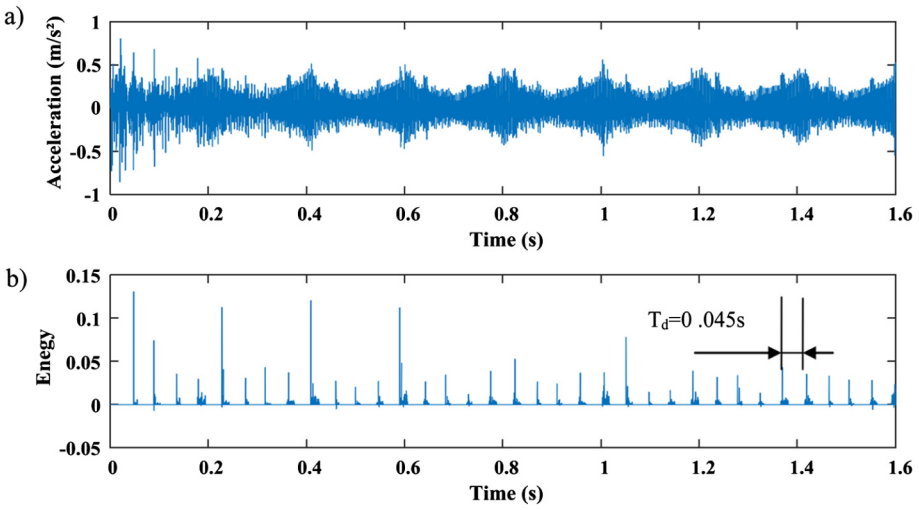

Fig. 18. Vibration signals of defect level 3 (10%) with 50% of rotational speed fluctuation: a) original signal; b) shock signal.

5. Conclusion

In this paper, we developed a fault diagnosis procedure based on the extraction of the shock content caused by a tooth defect from simulated vibration signals of a bevel gearbox running under variable speed and load. It is based on the Shock Detector (SD) method. In this approach, vibration signals are firstly decomposed by EMD, and then TKEO is applied to demodulate the most impulsive IMF. Afterwards, the shock detector is applied to the TKEO signal, which results in a filtered signal containing only shock components reflecting the presence of defects, removing all other random or harmonic components. This procedure was applied to diagnose a crack fault on one pinion tooth of a bevel gear transmission. Different levels of defect, 1%, 5%, and 10% were considered, with a fluctuation of the rotational speed of 5% and 50%. The obtained results proved that the proposed procedure has the ability to detect the presence of the gear fault at an early stage. Moreover, it showed a good robustness even with an important fluctuation of the rotational speed of 50%. As future work, we propose to study the tooth cracked defect, which could be introduced through shock equations.

References

[1] C.M. Vicuñan, F. Chaari, Analysis of a planetary gearbox under non-stationary operating conditions: numerical and experimental results, in: F. Chaari, R. Zimroz, W. Bartelmus, M. Haddar (Eds.), Advances in Condition Monitoring of Machinery in Non-Stationary Operations, 4th Int. Conf. on Condition Monitoring of Machinery in Non-Stationary Operations (CMMNO 2014), Lyon, France, 15 December 2014, in: Applied Condition Monitoring, Springer, Cham, Switzerland, 2016, pp. 351–362.

[2] R. Zimroz, W. Bartelmus, Gearbox condition estimation using cyclo-stationary properties of vibration signal, Key Eng. Mater. 413 (2009) 471–478.

[3] M. Cocconcelli, R. Zimroz, R. Rubini, W. Bartelmus, STFT based approach for ball bearing fault detection in a varying speed motor, in: T. Fakhfakh, W. Bartelmus, F. Chaari, R. Zimroz, M. Haddar (Eds.), Condition Monitoring of Machinery in Non-Stationary Operations, Springer, Berlin, Heidelberg, 2012, pp. 41–50.

[4] L. Hongmei, L. Lianfeng, M. Jian, Rolling bearing fault diagnosis based on STFT-deep learning and sound signals, Shock Vib. 2 (2016) 1–12, https://doi.org/10.1155/2016/6127479.

[5] R. Chaari, M.T. Khabou, M. Barkallah, F. Chaari, M. Haddar, Dynamic analysis of gearbox behaviour in milling process: non-stationary operations, Proc. Inst. Mech. Eng. C, J. Mech. 19 (2016) 3372–3388.

[6] K. Worden, W.J. Staszewski, J.J. Hensman, Natural computing for mechanical systems research: a tutorial overview, Mech. Syst. Signal Process. 25 (2011) 4–111.

[7] H. Li, Y. Zhang, Bearing faults diagnosis based on EMD and Wigner-Ville Distribution, in: Proceedings of the World Congress on Intelligent Control and Automation (WCICA), Dalian, China, 21–23 June 2006, pp. 5447–5451.

[8] J. Zhang, Z. Feng, Z. Qin, F. Chu, Gearbox fault diagnosis using time-wavelet energy spectral analysis, in: T. Fakhfakh, W. Bartelmus, F. Chaari, R. Zimroz, M. Haddar (Eds.), Condition Monitoring of Machinery in Non-Stationary Operations, Springer, Berlin, Heidelberg, 2012, pp. 223–230.

[9] K. Aharamuthu, E.P. Ayyasamy, Application of discrete wavelet transform and Zhao-Atlas-Marks transforms in non-stationary gear fault diagnosis, J. Mech. Sci. Technol. 27 (2013) 641–647.

[10] X. Cheng, X. Zhang, L. Zhao, A. Deng, Y. Bao, Y. Liu, Y. Jiang, The application of shuffled frog leaping algorithm to wavelet neural networks for acoustic emission source location, C. R. Mecanique 342 (4) (2014) 229–233.

[11] C. Junsheng, X.W. Ma, Y. Yang, Gear fault diagnosis method based on VPMCD and EMD, J. Vib. Shock 32 (2013) 9–13.

[12] Y. Lv, R. Yuan, G. Song, Multivariate empirical mode decomposition and its application to fault diagnosis of rolling bearing, Mech. Syst. Signal Process. 81 (2016) 219–234.

[13] R. Ziani, A. Felkaoui, R. Zegadi, Bearing fault diagnosis using multiclass support vector machines with binary particle swarm optimization and regularized Fisher's criterion, J. Intell. Manuf. 28 (2) (2017) 405–417.

[14] X. Yu, F. Dong, E. Ding, C. Fan, Rolling bearing fault diagnosis using modified LFDA and EMD with sensitive feature selection, IEEE Access 6 (2018) 3715–3730.

[15] Z. German-Sallo, H.S. Grif, Hilbert-Huang transform in fault detection, Procedia Manuf. 32 (2019) 591–595.

[16] D. Yu, Y. Yang, J. Cheng, Application of time–frequency entropy method based on Hilbert–Huang transform to gear fault diagnosis, Measurement 40 (2007) 823–830.

[17] F. Chaari, W. Baccar, M.S. Abbes, M. Haddar, Effect of spalling or tooth breakage on gearmesh stiffness and dynamic response of a one-stage spur gear transmission, Eur. J. Mech. A, Solids 27 (4) (2008) 691–705.

[18] H. Mahgoun, F. Chaari, A. Felkaoui, Detection of gear faults in variable rotating speed using variational mode decomposition (VMD), Mech. Ind. 17 (2) (2016) 207–221.

[19] B. Badri, M. Thomas, S. Sadok, A shock filter for bearing slipping detection and multiple damage diagnosis, Int. J. Mech. 5 (4) (2011) 318–326.

[20] T. Peng, Coupled Multi-Body Dynamic and Vibration Analysis of Hypoid and Bevel Geared Rotor System, Ph.D. Thesis, University of Cincinnati, OH, USA, 2010.

[21] M. Karray, F. Chaari, F. Viadero, A.F. del Rincon, M. Haddar, Dynamic response of single stage bevel gear transmission in presence of local damage, in: F. Viadero, M. Ceccarelli (Eds.), New Trends in Mechanism and Machine Science, Proc. 4th European Conference on Mechanism Science (EUCOMES 2012), Santander, Spain, 18–22 September 2012, in: Mechanisms and Machine Science, vol. 7, Springer, Dordrecht, Heidelberg, New York, London, 2013, pp. 337–345.

[22] V. Sharma, A. Parey, A review of gear fault diagnosis using various condition indicators, Proc. Eng. 144 (2015) 253–263.

[23] N.E. Huang, Z. Shen, S.R. Long, The empirical mode decomposition and the Hubert spectrum for nonlinear and non-stationary time series analysis, Proc. R. Soc. Lond. A 454 (1998) 903–995.

[24] X. Hu, S. Peng, W. Hwang, EMD revisited: a new understanding of the envelope and resolving the mode-mixing problem in AM-FM signals, IEEE Trans. Signal Process. 60 (3) (2012) 1075–1086.

[25] J.F. Kaiser, Some useful properties of Teager's energy operators, in: Proc. IEEE International Conference on Acoustics, Speech, and Signal Processing, Minneapolis, MN, USA, 27–30 April 1993, vol. 3, 1993, pp. 149–152.

[26] A.O. Boudraa, F. Salzensteinb, Teager–Kaiser energy methods for signal and image analysis: a review, Digit. Signal Process. 78 (2018) 1–38.